Trees (2022) 36:1039–1052
https://doi.org/10.1007/s00468-022-02271-7

ORIGINAL ARTICLE

Intra-annual isotope variations in tree rings reveal growth rhythms within the least rainy season of an ever-wet tropical forest

Jorge A. Giraldo[1] · Jorge I. del Valle[1] · Sebastián González-Caro[1] · Carlos A. Sierra[2,3]

Received: 5 December 2020 / Accepted: 20 January 2022 / Published online: 17 February 2022

Abstract

Key message **Isotope variation ($\delta^{18}O$) in wood suggests new insights on growth rhythms in trees growing in tropical forest with extremely high precipitation, without seasonal droughts or flooding.**

Abstract It is well known that growth-limiting factors such as seasonal droughts can induce periodicities in woody tissue formation of tropical trees. In regions without seasonal droughts or flooding but sufficient water for photosynthesis (ever-wet tropical forests), rhythmic growth has been previously reported; however, triggering factors remain little explored. Our objective was to establish tree-ring frequency and probable growing season by analysis of the intra-annual variability of isotopic ratios in cellulose ($\delta^{18}O_{cellulose}$ and $\delta^{13}C_{cellulose}$) and relationships with environmental variables in two tree species (*Humiriastrum procerum* and *Virola dixonii*) growing in an ever-wet tropical forest (Choco region of Colombia, precipitation 7200 mm year^{-1}, mean annual temperature 25.9 °C), located close to the Pacific Ocean at ca 3° 57′ 12.54″ N–76° 59′ 27.96″ W. Here, we report annual rhythmic growth evidenced by radiocarbon analysis, leaf phenology, dendrometer records, and stable-isotope variation in cellulose. All evidence points to the probable growing season occurring during the least rainy months for both species. While intra-annual $\delta^{18}O_{cellulose}$ values follow a rhythmic variation, $\delta^{13}C_{cellulose}$ variations show a less clear pattern, probably due to deciduity and remobilization of non-structural carbon stored in previous growing stages. Furthermore, $\delta^{18}O_{cellulose}$ covary with relative humidity, vapor pressure deficit, short-wave solar radiation, and temperature during the least rainy months. In contrast, $\delta^{13}C_{cellulose}$ values were not significantly correlated with environmental variables. Our results show that stable-isotope variations in tree rings, even under ever-wet conditions, are valuable for understanding drivers of tropical tree growth in such conditions.

Keywords Dendrochronology · Biogeographical *Chocó* region · Tropical trees · C isotopes · O isotopes

Introduction

Improving our understanding of how tropical trees grow and respond to environmental drivers, and produce growth rhythms, is essential to predict tropical forest dynamics to management and conservation strategies. Despite high variability in plant growth rates among species and environmental conditions, climate is commonly suggested as the main driver for tree growth (Fritts 1976). In particular, the seasonality of environmental variables triggers tree-growth rhythms (Fritts 1976; Schweingruber 1988, 2007). For example, annual growth rings in many tropical tree species could be explained by water availability and seasonality as limiting factors (Lisi et al. 2008; Groenendijk et al. 2014; Brienen et al. 2016; Silva et al. 2016; Schöngart et al. 2017). On one hand, some studies have shown seasonal droughts as a limiting factor of tree growth and forest productivity in most tropical ecosystems (Wagner et al. 2012; Esquivel-Muelbert et al. 2016). On the other hand, annual seasonal flooding, as in estuarine or riverine ecosystems, can induce annual ring formation (Callado et al. 2001; Schöngart et al. 2002; Menezes et al. 2003; del Valle et al. 2012; Parolin et al. 2016). Thus, either water deficit (i.e., drought)

Communicated by S. Leavitt .

✉ Jorge A. Giraldo
jagiral1@unal.edu.co

[1] Departamento de Ciencias Forestales, Universidad Nacional de Colombia, Medellín, Colombia

[2] Max Planck Institute for Biogeochemistry, Jena, Germany

[3] Swedish University of Agricultural Sciences, Uppsala, Sweden

or excess (i.e., flooding) may negatively affect tropical tree growth.

The presence of annual tree rings in tropical regions with high precipitation during the entire year and without apparent water deficit or periodic flooding (hereafter ever-wet tropical forests) (Fichtler et al. 2003; Moreno and del Valle 2015; Giraldo et al. 2020) challenges the aforementioned assumptions about the factors inducing annual ring formation in tropical trees. Whereas little is known about drivers triggering wood phenology and interannual growth variability in tropical ever-wet forests, some studies based on dendrometers have found the highest growth increment occurs during the least-rainy period, and synchronized leaf shedding occurs during the rainy season or with flushing new leaves in the early part of the least rainy season (Frankie et al. 1974; Hazlett 1987; Breitsprecher and Bethel 1990; O'Brien et al. 2008). In addition, remote sensing indicates an increase in canopy photosynthetic activity during the least-rainy period in Amazon wet forests (Green et al. 2020), implying a reduction in tree growth and forest productivity during the rainiest months, photosynthetically limited by both, high cloudiness and excess of precipitation (Restrepo-Coupe et al. 2013), and suggesting that light and water availability in concert drive tropical tree growth.

Although the interaction between light and water availability may drive tree-growth rhythms in tropical ever-wet forests, the physiological mechanisms behind tree-growth control under such conditions are poorly understood. To resolve these uncertainties, the variability in stable-isotope composition measured with high-resolution sampling (intra-ring sampling), together with dendrochronology techniques, would be helpful to differentiate physiological factors involved in tree growth (Evans and Schrag 2004; McCarroll and Loader 2004; Anchukaitis et al. 2008; Managave et al. 2010; Managave and Ramesh 2012; Van der Sleen et al. 2017; Rahman et al. 2019). In particular, stable-isotope composition of carbon ($\delta^{13}C$) and oxygen ($\delta^{18}O$) in tree-ring cellulose are complementary in providing evidence about the ecophysiological responses to environment variations (McCarroll and Loader 2004).

Isotopic composition of tree rings is not identical to the isotope composition of their sources of carbon and water due to the fractionation process during transport or incorporation in the plant tissue (Farquhar et al. 1982; Roden et al. 2000). However, the signal of the prevailing environmental conditions remains in tree-ring cellulose and constitutes a potential proxy for past physiological processes (McCarroll and Loader 2004; Van der Sleen et al. 2017; Rahman et al. 2019). Variation of $\delta^{18}O$ in tree-ring cellulose is the balance between the effect of the water source, known as the amount effect (rainfall and/or soil water/groundwater), and the evaporative enrichment during leaf transpiration. Evaporative enrichment depends on vapor pressure deficit (VPD), leaf transpiration rates, and the degree of oxygen exchange between exported sugars and stem water during cellulose synthesis (Roden and Ehleringer 2000; Roden et al. 2000).

Carbon isotope fractionation ($\Delta^{13}C$) at the leaf level depends on stomatal conductance (g_s) and the ratio of leaf intercellular and ambient CO_2 concentrations (C_i/C_a) (Cernusak et al. 2013). $^{12}CO_2$ molecules have higher diffusivity than $^{13}CO_2$ molecules resulting in a higher carboxylation rate of ^{12}C relative to ^{13}C. Therefore, if stomatal conductance is low (and/or rate of photosynthesis is high), the internal concentration of CO_2 in the leaf will be low, resulting in weak discrimination against ^{13}C, which leads to high $\delta^{13}C$ values in wood. Conversely, if stomatal conductance is high and/or the rate of CO_2 assimilation via photosynthesis is low, the high internal CO_2 concentration allows greater discrimination against ^{13}C, leading to low $\delta^{13}C$ values (Farquhar et al. 1982; Cernusak et al. 2013). Hence, the variation of $\delta^{13}C$ in tree rings is affected mainly by photosynthetic assimilation rate and stomatal conductance. In addition, some deciduous tree species that use non-structural carbon reserves (usually enriched in ^{13}C) under stress conditions can modify $\delta^{13}C$ values over the period of tree-ring formation (Helle and Schleser 2004; Ohashi et al. 2009; Cintra et al. 2019).

In previous observations in a Neotropical ever-wet forest in the *Chocó* region of Colombia (precipitation > 7000 mm $year^{-1}$), several species were found to have periodic growth rhythms evident in tree-ring structures (Giraldo et al. 2020). These growth rhythms were inferred by independent sources of evidence such as (1) annual tree-ring synchronization in multiple tree species, (2) intra-annual variability measured with dendrometers, and (3) radiocarbon tree-ring dating. Observations of both positive and negative growth responses to water and light availability suggest that both excess and deficiency of these growth factors are responsible for seasonal growth rhythms in some tree species (Giraldo et al. unpublished). Hence, isotope ratio analysis would be a complementary tool for understanding the ecophysiological strategies under ever-wet conditions, without apparent water deficit or flooding. We assumed that in the ever-wet tropical forest, tree growth is greater under low precipitation and high light availability (i.e., reduced cloudiness). On the one hand, we hypothesized that trees record the water source in the cellulose $\delta^{18}O$ variability differently: low values of $\delta^{18}O$ in the cellulose during the early and late growing season (i.e., slow or no growth) and higher values of $\delta^{18}O$ in the cellulose during the middle growing season (near the middle of the growth ring). Thus, we expected higher $\delta^{18}O$ enrichment during the least rainy season when precipitation decreases and light availably increases. On the other hand, we expected to find greater discrimination against ^{13}C (i.e., more negative $\delta^{13}C$ values), during limited growing periods with high rainfall or lower light availability. In this study, we aimed: (1) to establish tree-ring frequency, (2) probable growing season,

and (3) the intra-annual radial variability of $\delta^{13}C$ and $\delta^{18}O$ in tree rings of *Humiriastrum procerum* and *Virola dixonii*, sampled in a tropical ever-wet forest without droughts or flooding. In addition, (4) we assessed the relationships between isotope ratios of tree rings and environmental variables related to precipitation and light availability. To our knowledge, this is the first study on isotope signatures in tree rings under ever-wet conditions. We expect these analyses to provide new insights into the factors influencing tree growth under extreme rainfall amounts in tropical forests.

Methods

Study area

The *Chocó* biogeographic region is a strip of land along the Pacific coast in northern South America, which extends about 800 km from San Lorenzo, north of Ecuador, to the Colombia–Panama border, locally known as the Darién Gap (Diaz and Gast 2009). The boundaries of the region are delimited by the southernmost and northernmost mean positions of the Inter-Tropical Convergence Zone (ITCZ) where the trade winds converge. Driven by the seasonal cycle of solar insolation and carrying clouds and rain, every year the low-pressure ITCZ band migrates through this narrow strip from its southernmost position in January until reaching its northernmost position in July, followed by a return to the south (Yan 2005; Guzmán et al. 2014). Thus, towards the center of this region, where the study area is located, the rains induced by the low pressures from south to north are still falling when the low pressures from north to south arrive, and it rains again (del Valle 1994; Guzmán et al. 2014). This is the primary factor that makes this region the rainiest of the Americas. Another contributing factor to the high rainfall in this region is the existence two low-level jet streams, namely, the Caribbean and the *Chocó*'s (Poveda and Mesa 2000; Mesa and Rojo 2020). These two jet streams transport humidity from the Atlantic and the Pacific Oceans to the *Chocó* region, respectively. Finally, the proximity to the Pacific Ocean of both the coastal *Baudó* Range and the Western Andean Cordillera induces copious orographic rains throughout the region by the Föhn's effect (David et al. 2014; Urrea et al. 2019).

Climatologists have described the center of the *Chocó* as an aseasonal zone according to the mean rains of each month (Guzmán et al. 2014) or the daily rains (Urrea et al. 2019). In this aseasonal zone, there are 12 localities with records of more than 8000 mm of mean annual precipitation, 2 with more than 12,000 mm. The town of *López de Micay* (2.85° N, 77.25° W) receives more than 13,000 mm $year^{-1}$, the rainiest locality on Earth (Mesa and Rojo 2020). In our study area, around the Pedro Antonio Pineda Tropical Forest Center of the University of Tolima (3° 57′ 12.54″ N, 76° 59′ 27.96″ W) (Fig. 1), precipitation exceeds 7200 mm $year^{-1}$. According to the Gaussen xerothermic index (Bagnouls and Gaussen 1957) and the monthly potential evapotranspiration (Holdridge 1967), there are no dry months (Walter et al. 1976). The rainiest month is October with 805 mm (28 ± 2 rainy days), and the least rainy month is February with an average of 370 mm (19 ± 4 rainy days) (Fig. 1b, c), twice the potential evapotranspiration (127 mm). The mean temperature of all months deviates very little from the mean annual temperature of 25.9 °C (Fig. 1d). Small hills with slopes up to 45° are frequent, with elevations ranging from 40 to 100 m above sea level. Soil texture is dominantly classified as clay-loam. In addition, these soils are poor in nutrients with high iron and aluminum concentrations (Faber-Langendoen and Gentry 1991).

Sampled species

In November 2016, we sampled four cross-sectional disks: two individuals of *Humiriastrum procerum* (Humiriaceae), wood specific gravity 0.72, and two individuals of *Virola dixonii* (Myristicaceae), wood specific gravity 0.46 g cm^{-3}. All trees sampled were growing under similar conditions on small hills, as dominant trees ca. 15–20 m height in a closed canopy non-flooded forest of ca. 70 years of secondary succession. This forest is characterized by high tree species richness, but the number of individuals per species tends to be very low (Giraldo et al. 2020). In one hectare, Faber-Langendoen and Gentry (1991) found in these forests, 258 tree species and 675 individuals with a diameter at breast height ≥ 10 cm. As 675/258 gives 2.6 trees by each species, this implies that, on average, there are only 2–3 trees of the same species per hectare, individuals of the same species are commonly spaced ca. 50–400 m. This circumstance reduces the potential for sampling multiple individuals per species.

Both sampled species shed their leaves between August and October (*V. dixonii* is a semi-deciduous tree). Leaf flushing and new leaves are common from November to February. Little is known about flowering and fruit production of *V. dixonii*, but *H. procerum* flowering occurs from February–March (Personal observations between 2016 and 2021). The last tree ring in all samples was complete, and some of them had just begun to form new woody tissue (trees were sampled in November 2016). These facts allowed us to assume that the end of each annual tree ring for both species occurs in October, and the beginning of the new phenological year starts in November. In addition, based on herbarium records from Global Biodiversity Information Facility (https://www.gbif.org/species/), we found that the presence of both species is mainly restricted to wet forests of the northwestern region of South America (Ecuador and Colombia).

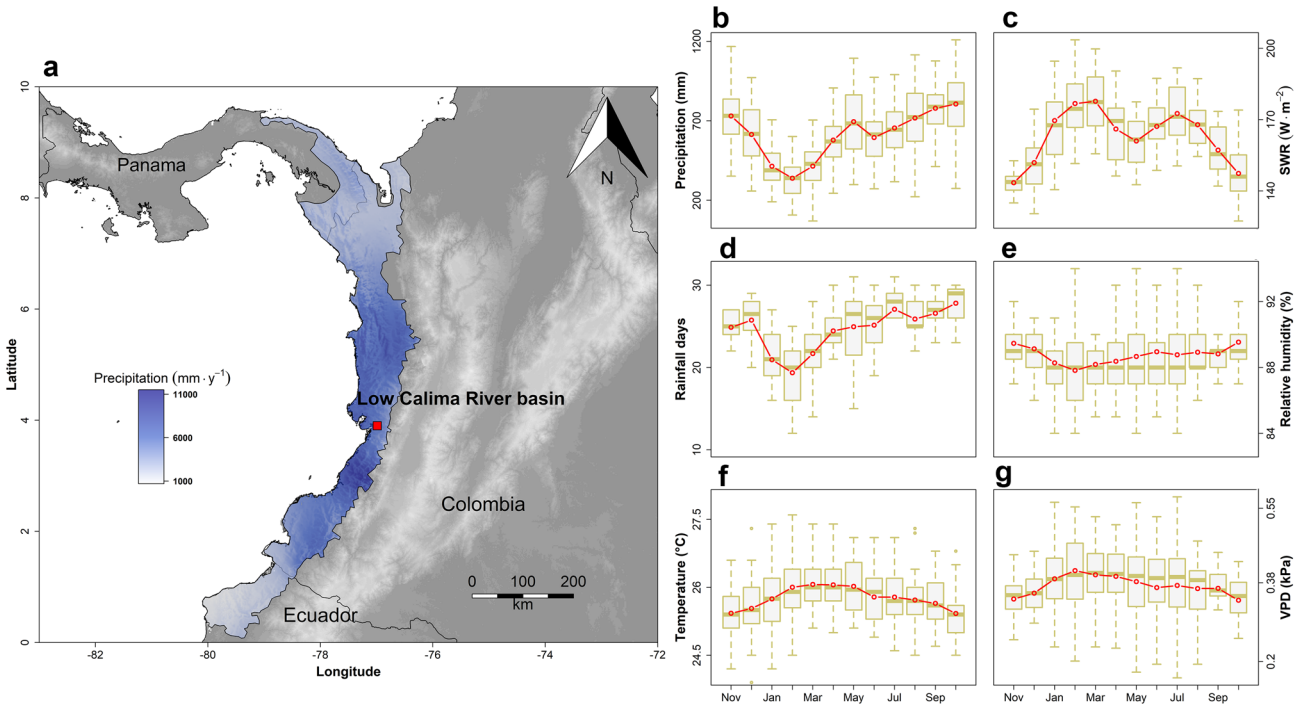

Fig. 1 **a** Study area in the Low *Calima* River Basin (square), located in the *Chocó* Region. The annual precipitation is shown based on CHELSA data (https://chelsa-climate.org/) (Karger et al. 2017). Mean monthly: **b** precipitation (mm). **c** Rainy days. **d** Temperature (°C), **e** incoming short-wave solar radiation SWR (W m^{-2}) available from Clouds and the Earth's Radiant Energy System—CERES (https://ceres.larc.nasa.gov/), **f** relative humidity (%), and **g** vapor pressure deficit VPD (kPa). Precipitation, rainy days, relative humidity and temperature were obtained from a meteorological station (IDEAM: http://www.ideam.gov.co/), VPD was calculated from the available data

Growing season based on dendrometer data

Between 2018 and 2019, we installed two automatic dendrometer bands (Tree-Hugger®, Global Change Solutions) in one individual per species included in this study. Both individuals were mature (diameter 17 and 27 cm) growing in similar conditions as sampled for isotope analysis. Measurements were recorded hourly, and data were downloaded every 5 weeks until the dendrometers failed. The damage was attributed to the harsh conditions the electric devices endured. However, such data allowed us to obtain additional information about the growing season for each species.

Tree-ring sampling and isotope variability

Growth rings of these two species are well defined in sanded disks (Fig. 2), characterized by the increase in cell wall thickness of fibers, producing an abrupt darker area on the outer edge of the rings (Fig. S1). In both species, wood is diffuse porous. We measured the tree-ring widths of each species (three radii for each cross-section). We compared tree-ring widths among individuals to ensure good crossdating. Next, we tested the formation frequency of tree rings using the radiocarbon bomb-peak method by sampling particular rings in each cross-section (Fig. 2a) (Fichtler et al. 2003; del Valle et al. 2014). We assumed a priori annual tree-ring formation and assigned the sampling year as the calendar year of the last complete ring formed (2016), and from there, we counted backwards to the pith. We collected about 20 mg of the wood for radiocarbon analyses from specific rings: 1991, 2001 and 2008 from *H. procerum* and 1989, 1992, 2001, 2004, from *V. dixoni*.

We used the software CaliBomb (Reimer et al. 2004) with North Hemisphere Zone 2 curve and one smoothing year function of CaliBomb to obtain the probable calendar dates from the radiocarbon values. The comparison between assumed calendar dates and calibrated dates from the radiocarbon analysis allowed us to establish the tree-ring formation frequency (del Valle et al. 2014). For the stable-isotope analysis, we cut one small block of wood *ca.* 5-mm wide and 10-mm high from each cross-section containing the last five growth rings closest to the bark (Fig. 2b). After a clear identification of the boundaries of the rings, we used a scalpel to slice 0.6 to 0.8-mm-thick segments progressively from the inside toward the outside of each ring (Fig. 2b). This method allowed us to divide each growth ring into a different number of slices (Table S1). Each slice was placed in labeled Eppendorf tubes for the individual cellulose extraction process.

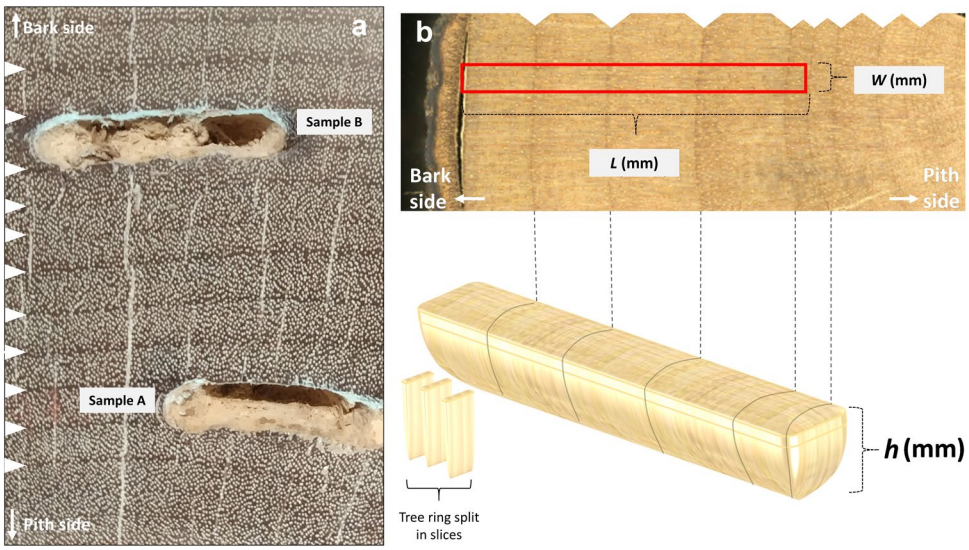

Fig. 2 Wood samples for radiocarbon and stable isotopes analysis. **a** Two sampled tree rings for radiocarbon analysis in one cross-section of *Humiriastrum procerum,* Sample A and B: An innermost and the outermost tree ring, respectively. **b** A rectangular section used for cellulose extraction, and the analyses of stable isotopes in one cross-section of *Virola dixonii. L* is the length of the section in mm (the value of *L* is variable among trees, depending on the last five tree-ring widths). The width of the rectangular section was 5 mm. The height (*h*) of rectangular sections was 10 mm. We obtained the slices with a scalpel and a stereomicroscope. The arrows on the edge of the images indicate the growth-ring boundaries

Cellulose was extracted from individual wood samples (both for radiocarbon and stable-isotope analysis) at the Radiocarbon Laboratory of the Max Planck Institute for Biogeochemistry, following the protocol described by Steinhof et al. (2017). The first and last procedure involves extracting the samples in a Soxhlet for 12 h with toluene–isopropanol (1:1) and HO, respectively. The intermediate steps include oxidation of lignin in an acidified solution ($NaClO_2$, CH_3COOH) and digestion of hemicelluloses using an alkaline solution (NaOH) in micro-filter funnels held in a multiport batch-processing manifold (temperature 65–70 °C), which facilitated the bleaching of the samples and transforming them to pure α-cellulose.

We weighed cellulose samples (0.51–1.01 mg for $^{13}C/^{12}C$ and 0.51–0.64 mg for $^{18}O/^{16}O$) in silver capsules, and the isotopic compositions ($\delta^{18}O$ and $\delta^{13}C$) were measured using a Thermo Fisher TC/EA oven coupled to a Delta + XL mass spectrometer at the Laboratory of Stable Isotopes of the Max Planck Institute for Biogeochemistry, Jena, Germany. This Laboratory uses internal standards calibrated with Vienna Mean Standard Ocean Water (VSMOW), Standard Light Antarctic Precipitation (SLAP) and Vienna Pee Dee Belemnite (VPDB). Samples were standardized against in-house standards: IAEA-601 ($\delta^{18}O$: 22.93‰) Acetanilide ($\delta^{13}C$: − 30.06‰) and Caffeine ($\delta^{13}C$: − 40.46‰) (Werner and Brand 2001; Brand et al. 2009). The proportion of isotopes were expressed in delta (δ) notation, relative to the international standards, VSMOW for oxygen, VPDB for carbon, as [$\delta^{18}O$ or $\delta^{13}C$ (‰) = $(R_{sample}/R_{standard} - 1) \times 1000$], where R_{sample} and $R_{standard}$ are the proportions of the heavy isotope versus the light isotope, for the sample and the standard, respectively. Given the small variation in the isotopic ratios of the samples with respect to those of the standards, they are expressed in values per thousand (‰, per mil) (Van der Sleen et al. 2017). The analytical error (1σ) of $\delta^{18}O$ and $\delta^{13}C$ was within 0.2‰.

Environmental data

Monthly records of precipitation (mm), temperature (°C), rainfall days, and relative humidity (%) were available from the *Bajo Calima* Meteorological Station (IDEAM, http://www.ideam.gov.co/) from 1972 to 2016. We also calculated the monthly air vapor pressure deficit: VPD (kPa) based on the temperature and the relative humidity for the available period. Due to the lack of ground instrumental measurements of solar radiation, we used the mean monthly shortwave solar radiation (SWR W m^{-2}) between 2000 and 2019 from Clouds and the Earth's Radiant Energy System—CERES datasets (https://ceres.larc.nasa.gov/) (Kato et al. 2013).

Assessing amount effect in rainfall

In our study site, there is no isotopic information on rainwater (e.g., $\delta^{18}O_{precipitation}$). However, to assess if

the amount effect exists in our study area, we used the database of the Global Network of Isotopes in Precipitation (GNIP) of the International Atomic Energy Agency (IAEA). This network has just one data point in the *Chocó* Region (*Tulenapa*, *Urabá*, *Colombia*). Although *Tulenapa* is less rainy than our study area, the source of rainfall in the region is the same. To check this, we compare *Tulenapa* and *Bajo Calima* precipitation, graphically and via correlation. We ran a correlation between rainfall and $\delta^{18}O_{precipitation}$ for *Tulenapa* to establish the existence of the amount effect in this region. We also selected a pool of data ($\delta^{18}O_{precipitation}$ vs. precipitation) from other GNIP lowland tropical areas around the World, characterized by high rainfall (over 2300 mm year^{-1}). Then, we ran a correlation ($\delta^{18}O_{precipitation}$ vs. precipitation) for the complete dataset using the monthly precipitation values higher than 100 mm month^{-1} to determine the effect of different precipitation levels and to establish the existence of the amount effect in similar ever-wet tropical areas.

Data analysis

To assess our predictions, we correlated isotope ratios ($\delta^{18}O$ and $\delta^{13}C$) across tree rings with environmental variables. First, we used the mean monthly records for precipitation (*P* mm), vapor pressure deficit (VPD kPa), shortwave solar radiation (SW Wm^{-2}), and relative humidity (RH %) as environmental predictors of our hypotheses. We also included minimum temperature (Tmin °C), maximum temperature (Tmax °C), average temperature (Tmean °C) to assess potential thermal effects on $\delta^{18}O$ and $\delta^{13}C$ variation across tree rings. We ordered the months according to the entire phenological year for each tree species (i.e., tree ring starts after leaf flushing in November and ends in October with the leaf shedding). We grouped the isotopic composition in two classes, within and boundary ring, which represent the middle and early plus late growing season, respectively. This scheme focuses on variability of isotopic composition across tree rings in only part of the growing season and facilitates assigning climatic data for each growing period. For this, we separated isotope values for each tree ring in four quarters relative to the growing season (tree rings). We assumed the average of the first and fourth quarter isotopic ratios within tree rings represent isotopic ratios at ring boundaries ($\delta^{18}O_{rb}$ and $\delta^{13}C_{rb}$) corresponding to the early and late growing season. In addition, the isotopic ratio of the middle growing season was calculated as the average between the second and third quarters (isotopic ratios within rings: $\delta^{18}O_{wr}$ and $\delta^{13}C_{wr}$). Finally, we used the Pearson correlation test to assess the relationship between isotope series of four sampled radii (two individuals per species) and environmental variables.

Results

Tree-ring frequency

We tested the isotopic signature of ^{14}C of different tree rings in all cross-sections. The ^{14}C results in the $F^{14}C$ metric and their calibrations in the calendar years are presented in Table 1. The number of years between calibrated dates was the same as the tree-ring number between radiocarbon sampled rings; this fact confirms the annual nature of the tree rings in the sampled species (Table 1). According to this result, tree rings marked and counted allow us to know the real age of trees. In addition, crossdating was successful between the tree-ring series sampled for each species (Fig S2). We found mean significant serial intercorrelation values of 0.48 for *H. procerum* and 0.41 for *V. dixonii* (p value < 0.05 in both cases). The series intercorrelations represent the common-level signal recorded in tree rings for the available tree samples: too few for developing a chronology, but enough to confirm our stable-isotope observations.

Radial increment during growing season

Our dendrometer measurements between 2018 and 2020 (Fig. 3) provide complementary evidence to our previous observations of leaf phenology. In both species, radial increment growth began after a decrease in rainfall (October) and fast conspicuous growth during the least rainy months (November–March), when new leaves have matured in both species.

Intra-annual variability of $\delta^{13}C$ and $\delta^{18}O$ across tree rings

We observed a cyclic pattern of $\delta^{18}O$ ratios in tree rings: high values within tree rings (middle growing season) and low values tending to coincide with the end of the growing season (tree-ring boundaries) (Fig. 4). Such seasonal variation is similar in the two individuals of *H. procerum* (Fig. 4b), but not so clear in one individual of *V. dixonii* (Fig. 4b). Variability of $\delta^{13}C$ is observed within rings of *H. procerum* and *V. dixonii*, but there is no consistent pattern (Fig. 4c, d). The intra-annual variation of $\delta^{18}O$ for *H. procerum* was from 20.7 to 29.5‰ and from 21.8 to 28.3‰ for *V. dixonii* (Fig. 4e, f). The range of $\delta^{13}C$ values was less pronounced and ranged from − 29.5 to − 28.1‰ in *H. procerum*, and from − 30.6 to − 27.2‰ in *V. dixonii* (Fig. 4g, h). In *H. procerum,* the local minimum values of $\delta^{18}O$ coincided with the end tree-ring boundaries (Fig. 4a dashed lines). In both species, the highest values of $\delta^{13}C$ tend to occur within the tree ring and start to decrease until

Table 1 Results of ^{14}C dating and calibration in calendar dates of the seven-particular tree ring from four trees

Tree species	Sample ID	DBH (cm)	Height (m)	Radiocarbon sample	$F^{14}C$	Calibrated age range (1σ)	CaliBomb calibrated age range (2σ)	Cal AD	Years between dated samples	Tree-rings between dated samples	Tree age (years)
Humiriastrum procerum	Hpro65	56.5	20	A	1.1482 ± 0.0019	[1990.7–1991.96] (1.0)	[1990.38 + 1992.63] (0.94)	1991	10	10	36
	Hpro65	56.5	20	B	1.0881 ± 0.0016	[2000.75–2001.94] (1.0)	[2000.28–2002.61] (0.942)	2001			
	Hpro82[a]	29.9	18	A	1.0578 ± 0.0020	[2006.98–2008.87] (0.96)	[2005.88–2009.24] (0.89)	2008	8[a]	8[a]	43
Virola dixonii	Vdix43	13.4	15	A	1.088 ± 0.00180	[2000.75–2001.98] (1.0)	[2000.26–2002.66] (0.941)	2001	2	2	36
	Vdix43	13.4	15	B	1.0749 ± 0.0021	[2003.02–2004.65] (1.0)	[2002.34–2005.16] (0.926)	2004			
	Vdix199	22.98	18	A	1.1717 ± 0.0021	[1988.46–1989.54] (1.0)	[1988.06–1990.00] (0.924)	1989	3	3	36
	Vdix199	22.98	18	B	1.1395 ± 0.0020	[1991.85–1993.16] (1.0)	[1991.08–1993.55] (0.950)	1992			

Calibrated ages were obtained from the CaliBomb software (Reimer et al. 2004) using the bomb curve of the Northern Hemisphere Zone Two (NHZ2, Hua et al. 2013). DBH: diameter at breast height. $F^{14}C$: fraction modern of ^{14}C (Postbomb). Calibrated date with 1σ and 2σ (Prob): mean calibrated age range, with 1 sigma and 2 sigma, values in parentheses indicate percent probability given by CaliBomb. The lowest probabilities are not included (see radiocarbon calibration section in supplementary information). Cal AD: mean calibrated age rounded to the first integer calendar year. Years between dated samples: the number of years between Cal AD from the same tree. Tree-rings between dated samples: the number of tree rings between Cal AD from the same tree. Tree age: number of annual tree rings in the cross-section

[a]One single tree ring dated by radiocarbon. The difference between the dates and tree-ring number was estimated with the last complete ring (2016)

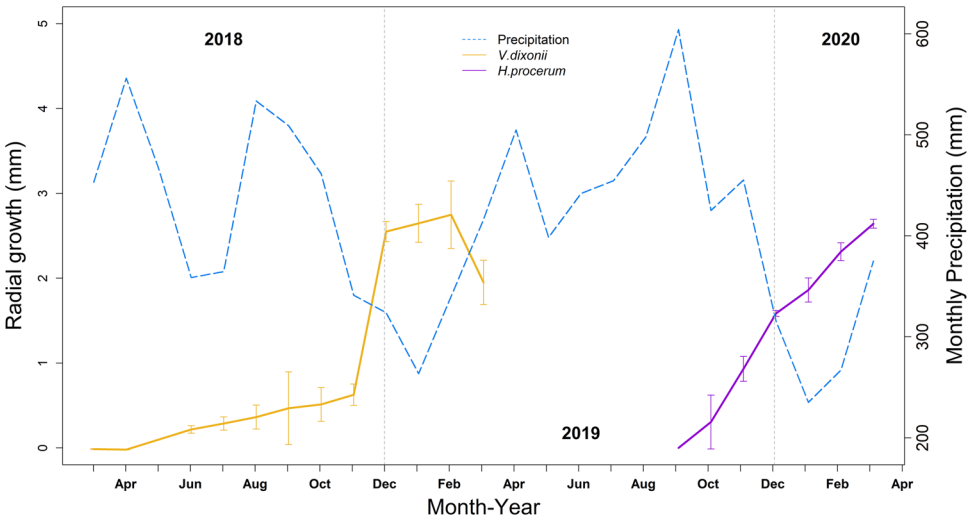

Fig. 3 Radial growth observations (mm) vs. precipitation (mm). Curves with bars (variability) represent the cumulative mean monthly radial growth of the trees. The dashed line corresponds to mean monthly precipitation. Measurements were performed hourly and averaged monthly: from March 28, 2018, to April 5, 2019 (*Virola dixonii*) and from September 25, 2019, to 14 March 2020 (*Humiriastrum procerum*)

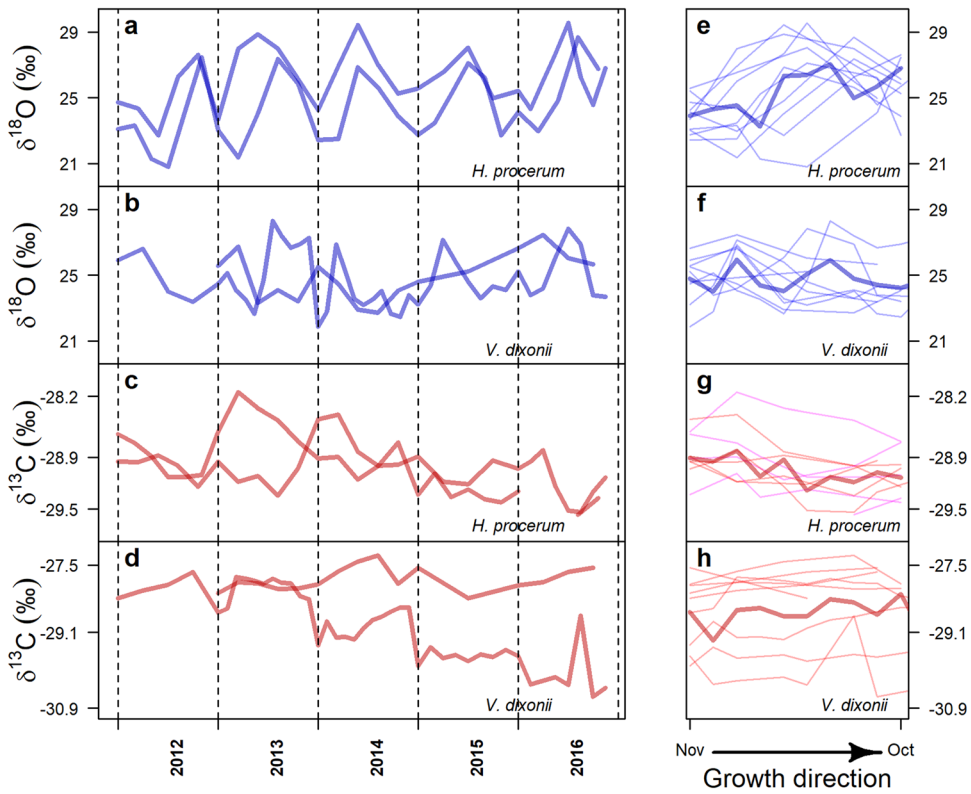

Fig. 4 **a**–**d** Intra-annual variations of $\delta^{18}O$ (blue lines) and $\delta^{13}C$ (red lines) of all rings of the two *Humiriastrum procerum* trees and two *Virola dixonii* trees for 2012–2016. **e**–**h** The mean annual isotope pattern of this period for each species (bold lines) and the isotope patterns of each of the years (thin lines)

reaching a late growing season minimum (late growing season). These facts suggest non-random patterns for the $\delta^{18}O_{cellulose}$, which are consistent with our expectations. However, the intra-annual variation of $\delta^{13}C_{cellulose}$ does not show such a clear pattern (Fig. 4).

Amount effect in rainfall

Due to a lack of data on the isotopic composition of rain in our study area, we explored the amount effect for the tropical humid forest with data from the GNIP database. *Tulenapa* is the only locality within *Chocó* region with isotopic information on rainwater. We found similar patterns of mean monthly precipitation between *Bajo Calima* and *Tulenapa* localities ($r = 0.82$, p value < 0.05) (Fig. S3a). We found a negative correlation between $\delta^{18}O$ in the rain and the monthly rainfall for *Tulenapa* ($r = -0.83$, p value < 0.05, $n = 12$) which suggests the existence of the amount effect in this locality, also assumed for the *Bajo Calima* locality (Fig. S3b-c). The correlation between $\delta^{18}O$ in the rainwater and

the monthly rainfall for other high rainfall humid lowland tropics is also negative for the complete dataset ($r = -0.36$, p value < 0.05, $n = 154$), the subset using only precipitation values higher than 100 mm month^{-1} ($r = -0.30$, p value < 0.05, $n = 145$) (Fig. S3c).

Correlations between isotopic ratio and environmental variables

We found significant correlations (i.e., $p < 0.05$) between $\delta^{18}O$ isotopic values at both the ring boundary ($\delta^{18}O_{rb}$) and within tree ring ($\delta^{18}O_{wr}$), with monthly environmental variables (*P*, RH, VPD, SWR, Tmean, Tmax, and Tmin) (Fig. 5). The $\delta^{18}O_{wr}$ values, which represents isotopic composition for the middle of growing season, were correlated ($p < 0.05$) with RH (February: $r = 0.47$), VPD (February: $r = -0.46$), SWR (November: $r = 0.48$), and Tmean (December: $r = 0.47$, January: $r = 0.44$ and November to January: $r = 0.45$) (Fig. 5). We also observed significant correlations between $\delta^{18}O$ isotopic ratios at ring boundaries ($\delta^{18}O_{rb}$) and PP (November: $r = 0.50$, May: $r = 0.50$, August: $r = 0.52$ and, August to October: $r = 0.45$), RH (December: $r = 0.56$), VPD (December: $r = -0.45$), SWR (May: $r = -0.47$ June: $r = -0.56$, July: $r = -0.54$, and both November to January: $r = 0.45$ and May to July: $r = -0.54$), Tmean (June: $r = -0.47$, July: $r = -0.52$ and May to July: $r = -0.47$), Tmin (January: $r = -0.47$, February: $r = 0.45$, April: $r = -0.5$ and, August: $r = -0.47$), Tmax (September: $r = -0.49$ and August to October: $r = -0.51$). In contrast, carbon isotopic ratios from cellulose were not significatively correlated with environmental variables (Fig. S4).

Discussion

Here, we reported annual tree rings and intra-annual isotopic signals of from two tree species growing under ever-wet conditions. Our results are novel and challenge current assumptions about tropical tree-ring formation and the effect of environmental conditions on tree growth (Brienen et al. 2016). On the one hand, our evidence on tree-ring frequency, leaf phenology, and dendrometer records allow us to describe the growing season for the two tree species in this study. Radial tree growth rapidly increases as rainfall decreases, in contrast to the observed pattern in seasonally tropical dry forest or water-limited ecosystems (Lisi et al. 2008; Mendivelso et al. 2016). On the other hand, we found that isotopic ratios, mainly for $\delta^{18}O$, covary with the intra-annual variation of relative humidity, vapor pressure deficit, short-wave solar radiation, and temperature in both the ring boundary and within the tree ring (Fig. 5). Although there are similar isotopic studies in the tropics (Van der Sleen et al. 2015, 2017), to our knowledge, this is the first study of isotopic ratio variation in tropical ever-wet forests.

Our study explores the growth rhythms of the little-studied ever-wet tropical forest in the *Chocó* region. Our phenological observations evidenced that leaf shedding coincides with the wettest period (August–October), which is also the lowest insolation period (i.e., low light availability and high cloudiness) (Fig. 1). This evidence suggests ring boundary formation occurs between these periods. We observed the last ring boundary of sampled trees was complete by November 2016 (sampling date). Such observations explain the annual pattern in tree growth. Moreover, both studied species evidenced the highest radial increment during January to March (Fig. 3). In that period, there is a marked increase in insolation, which coincides with the least-rainy season (i.e., less cloudiness and high light availability) (Fig. 1). In the absence of a distinct day-length signal, dry season, or seasonal temperature changes at the study site, tree species might adapt phenology, and consequently growth rhythms, to the annual course of daily insolation (Calle et al. 2010; Borchert et al. 2015). In addition, endogenous control of growth rhythm should be considered as a possible trigger in tropical tree species from the ever-wet forest (Baker et al. 2017).

The $\delta^{18}O$ signature in cellulose helps identify annual rings and is more effective than $\delta^{13}C$ (Ohashi et al. 2016; Van der Sleen et al. 2017). While we were able to identify tree-ring boundaries in both species, we observed periodic $\delta^{18}O$ signatures that coincided with the border of the rings and higher values within tree rings (Fig. 4). Some authors claim that the growth ring delimitation through isotopic signatures is possible only if the annual precipitation pattern is strongly expressed (Managave and Ramesh 2012; Ohashi et al. 2016; Van der Sleen et al. 2017). They suggest few or no isotope signatures in areas where rain falls throughout the year. However, we found that some tree species can express variations in the $\delta^{18}O$ signature of tree-ring cellulose even under ever-wet conditions. The amplitudes of the intra-annual variation of $\delta^{18}O$ and $\delta^{13}C$ in *H. procerum* are 8.7‰ and 1.41‰, respectively. The magnitude of this amplitude is similar to that reported by other authors for species that grow in climates with high seasonal rainfall changes (Pons and Helle 2011; Ohashi et al. 2016; Cintra et al. 2019).

According to our hypothesis, the highest values of cellulose $\delta^{18}O$ occur within the tree rings (Fig. 4a, b). This part of the ring section approximately represents the middle of the growing season when the tree-growth rate is higher (Fig. 3). In addition, the middle of the growing season is characterized by the less-rainy months (Fig. 3) in which environmental $\delta^{18}O$ is high and can magnify tree $\delta^{18}O$ enrichment by amount effect (Fig S3) (Risi et al. 2008; Managave and Ramesh 2012). In contrast, lower values of $\delta^{18}O$ tend to occur close to ring boundaries

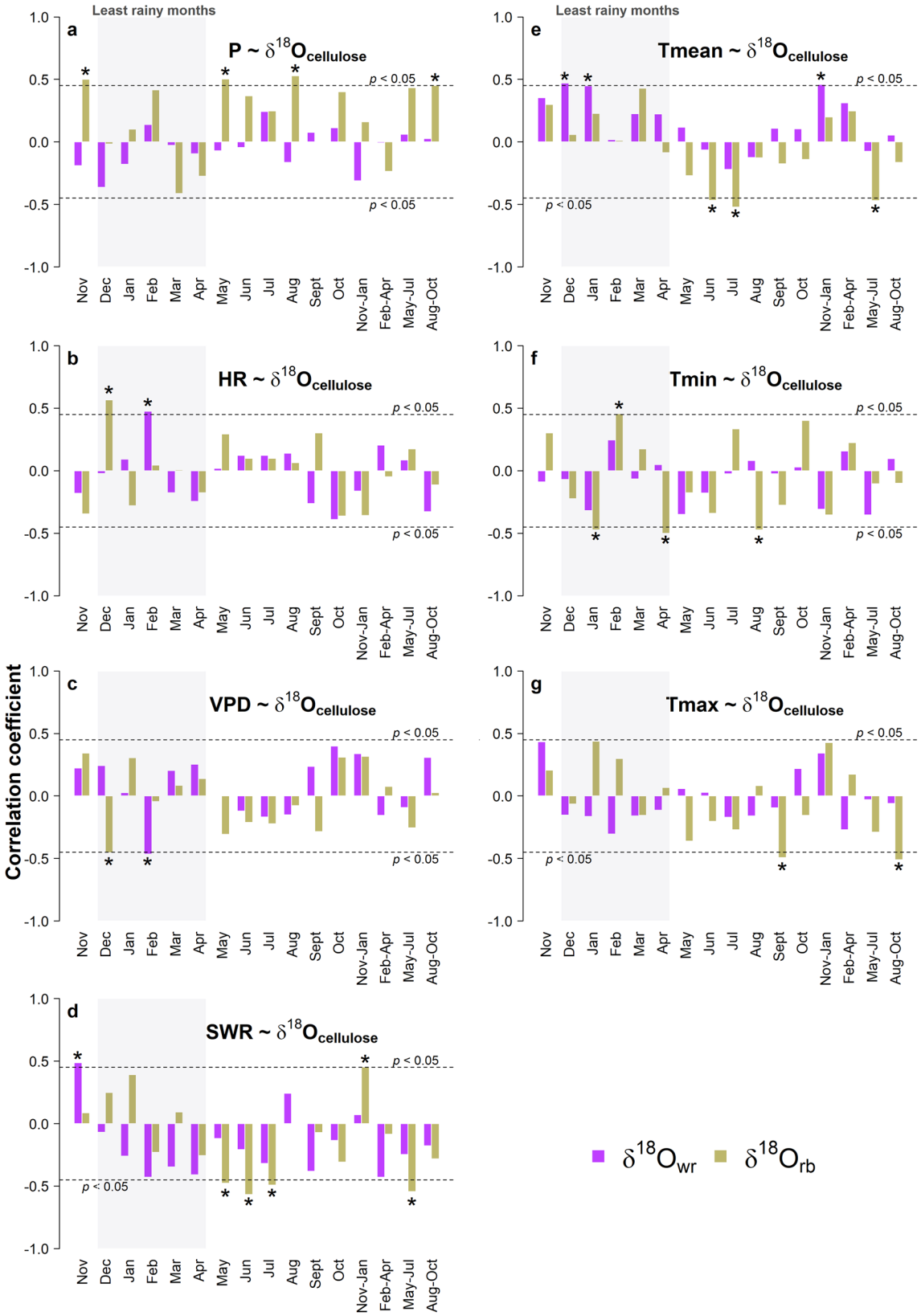
Least rainy months
a
P ~ δ18Ocellulose
b
HR ~ δ18Ocellulose
c
VPD ~ δ18Ocellulose
d
SWR ~ δ18Ocellulose
e
Tmean ~ δ18Ocellulose
f
Tmin ~ δ18Ocellulose
g
Tmax ~ δ18Ocellulose
p < 0.05
Correlation coefficient
1.0
0.5
0.0
-0.5
-1.0
Nov
Dec
Jan
Feb
Mar
Apr
May
Jun
Jul
Aug
Sept
Oct
Nov-Jan
Feb-Apr
May-Jul
Aug-Oct
δ18Owr
δ18Orb

◂**Fig. 5** The Pearson's correlation coefficients of the $\delta^{18}O_{cellulose}$ versus environmental variables (mean monthly and quarterly means). $\delta^{18}O_{rb}$: average of early and late $\delta^{18}O_{cellulose}$ (rb: ring boundaries), $\delta^{18}O_{wr}$: average of $\delta^{18}O_{cellulose}$ during the main growing season (wr: within the ring): **a** $\delta^{18}O_{wr}$ and $\delta 18O_{rb}$ vs P: precipitation (mm), **b** $\delta^{18}O_{wr}$ and $\delta^{18}O_{rb}$ vs HR: relative humidity (%), **c** $\delta^{18}O_{wr}$ and $\delta^{18}O_{rb}$ vs VPD: vapor pressure deficit (kPa), **d** $\delta^{18}O_{wr}$ and $\delta^{18}O_{rb}$ vs SWR: short-wave radiation (W m^2), **e–g** $\delta^{18}O_{wr}$ and $\delta^{18}O_{rb}$ vs Tmean—Tmin—Tmax; average of mean, minimum, and maximum monthly temperature, respectively (°C). $*p < 0.05$. The shaded region highlights the least rainy months ($p < 600$ mm $month^{-1}$)

(early + late growing season; Fig. 3), where tree-growth rate is slow due to leaf turnover. Leaf shedding occurs during the rainiest and lowest solar radiation months, probably to avoid excess leaf wetness and light deficit that reduces photosynthesis and increases energetic costs (Green et al. 2020). In addition, low VPD can reduce leaf photosynthetic capacity, affecting stomatal functioning, to maintain adequate water status and probably promoting leaf shedding (Aliniaeifard et al. 2014; Oksanen et al. 2018).

The observed positive correlations between $\delta^{18}O_{wr}$ and monthly relative humidity, short-wave radiation, and mean temperature occur during the less-rainy months (Fig. 5) when the tree-growth rate is higher (Fig. 3). However, we did not find a correlation of $\delta^{18}O_{wr}$ with monthly precipitation, but also, $\delta^{18}O_{rb}$ positively correlated with high precipitation (August–October quarter). These results may suggest that $\delta^{18}O$ leaf enrichment is not directly related to high transpiration rates and could be related to non-structural carbohydrate remobilization (i.e., starch or sugar) in the wettest period (Voelker and Meinzer 2017). Furthermore, we found a weak negative correlation of $\delta^{18}O_{wr}$ and $\delta^{18}O_{rb}$ with the vapor pressure deficit (VPD) during the less-rainy periods (Fig. 5), contrary to our expectations. During the tree-growth period (i.e., the least rainy season), high stomatal conductance and transpiration should lead to isotope enrichment; however, high air relative humidity reduces water loss gradient from the leaf to air, suppressing enrichment and adding H_2O isotopes by foliar water uptake (Goldsmith et al. 2017; Lehmann et al. 2018; Siegwolf et al. 2021). In addition, high air RH is related with cloudiness and fog conditions that commonly reduce light availability and air temperature. In this way, the $\delta^{18}O$ of atmospheric water vapor could modulate $\delta^{18}O$ of the leaf water, the source water's isotopic signal, and ultimately the $\delta^{18}O_{cellulose}$ (Siegwolf et al. 2021). This process is underestimated in previous studies because measurements under high air relative humidity conditions and low VPD are scarce (Goldsmith et al. 2017; Lehmann et al. 2018). Siegwolf et al. (2021) warn that the plant responses may contradict the current isotopic model fractionation under extreme conditions by not considering other fractionation mechanisms of the leaf- and stem-level processes.

Other studies showed that under continuous high soil moisture, high VPD can increase transpiration and, ultimately, photosynthesis (Huete et al. 2006; Restrepo-Coupe et al. 2013; Green et al. 2020). High transpiration rate under high VPD helps to reduce continuous leaf wetness that negatively affects the efficiency of photosynthesis and facilitate pathogen attacks (Oksanen et al. 2018). On the one hand, continuous leaf wetness stimulates stomata closure, reduces carbon assimilation rates and intracellular CO_2 concentration, and indeed can produce chronic damage to the photosynthetic apparatus (Ishibashi and Terashima 1995). Some studies have shown that fungal pathogens survive better under VPD lower than 0.43 kPa. In the study region, VPD rarely excess 0.4 kPa, suitable environmental conditions to pathogen development and infestation promoting leaf damage that can ultimately reduce photosynthesis (Prenger and Ling 2001). In addition, the possible non-structural carbohydrate remobilization may be related to photosynthetic tissue protection and secondary metabolites to reduce pathogen attack. The effect of leaf wetness on photosynthetic rates in ever-wet forests and the mechanisms to reduce it should be tested using experimental approaches.

According to our hypothesis, in both species, the lowest values of $\delta^{13}C$ tend to occur close to ring boundaries. In addition, the highest values of $\delta^{13}C$ tend to appear within the tree ring, but this signal is quite variable. Such variation of $\delta^{13}C$ could be attributable to remobilization of non-structural carbon (starch, soluble sugars, and lipids) stored during the growing season, which helps to maintain tree metabolic functions during periods of carbon limitation (Herrera-Ramírez et al. 2021), implying a post-photosynthetic fractionation of carbon isotopes (Helle and Schleser 2004; Ohashi et al. 2009; Cernusak et al. 2013). Although, our two species are deciduous, it is probable that the sampled trees do not experience severe stress or abrupt environmental changes that influence their photosynthetic rate. This is in contrast to the conspicuous seasonal variations of $\delta^{13}C$ often occurring in trees growing in seasonally dry forests (water-limited) (Poussart et al. 2004; Ohashi et al. 2009).

Our analyses of stable isotopes are limited by sampling methods and the number of samples. In particular, during sectioning of wood samples with a scalpel, the thickness of the slices is difficult to control and standardize. In addition, the curvature inherent to the growth layers can induce errors in dividing the sample into thin sections (Ohashi et al. 2009). We are aware that the isotopic signature is based on data from only 5 years and with samples taken from four individuals, two individuals per species. This limits the generalization of our results but motivates future work to establish general patterns. Measurements of $\delta^{18}O$ in both local precipitation and soil water, to link with the environmental $\delta^{18}O$ into cellulose, should be one of the most important tasks for future research.

Our study has confirmed annual growth rings in two tree species from the ever-wet forests of the Colombian Pacific: *Humiriastrum procerum* and *Virola dixonii*. The cyclic variations of $\delta^{18}O_{cellulose}$ were confirmed, according to our expectations. However, it remains unclear which processes dominate the $\delta^{18}O_{cellulose}$: variation of $\delta^{18}O$ from source water, leaf water enrichment or the $\delta^{18}O$ of atmospheric water vapor (high air relative humidity). Although the intra-annual variation of $\delta^{13}C_{cellulose}$ was less conspicuous and uncorrelated with environmental variables, we did not rule out the role of carbon remobilization from non-structural carbon in observed $\delta^{13}C_{cellulose}$. Additional research is needed to expand this work to other species and obtain more information on source water isotope endmembers. In particular, it would be useful to perform isotopic measurements of the meteoric water source. Despite the low environmental variability and highly humid conditions, high-resolution isotope variation in cellulose has proven valuable for understanding drivers of tree growth. The isotope rhythms in the tree rings also serve as a basis for delineating growing seasons, and may be useful for other species in the region, whose rings may be even less visibly distinct.

Author contribution statement JIDV, CAS and JAG contributed study conception and design. Data acquisition and statistical analysis were conducted by JAG and SGC. JAG wrote the draft of the manuscript and JIDV, CAS and SGC reviewed, commented, corrected, and edited the text. All the authors discussed and agreed to the final version.

Supplementary Information The online version contains supplementary material available at https://doi.org/10.1007/s00468-022-02271-7.

Acknowledgements We would like to thank the IsoLab and ^{14}C Analysis Facility of Max Planck Institute for Biogeochemistry for sample processing. In addition, we thank the "Tropical Dendroecology Laboratory" of the Department of Forest Sciences of the National University of Colombia and MEDEL Herbarium. We thank "Pedro Antonio Pineda Tropical Forestry Center" of the University of Tolima and those people who help us during sampling: Amalia Forero, Faber Hernández, Sixto Cáseres, Iris Valencia, Andrés Caro, Diego Andrés David, and Jorge Mario Velez. We also thank the Communicating Editor, and three anonymous reviewers whose comments help to improve our paper manuscript.

Funding Colciencias Project 1118-714-51372. Max Planck Institute for Biogeochemistry, JAG and SGC are supported by Colciencias in the announcement 785.

Availability of data and material Supplementary Information.

Declarations

Conflict of interest The authors declare that they have no conflict of interest.

References

Aliniaeifard S, Malcolm Matamoros P, van Meeteren U (2014) Stomatal malfunctioning under low VPD conditions: induced by alterations in stomatal morphology and leaf anatomy or in the ABA signaling? Physiol Plant 152:688–699. https://doi.org/10.1111/ppl.12216

Anchukaitis KJ, Evans MN, Wheelwright NT, Schrag DP (2008) Stable isotope chronology and climate signal calibration in neotropical montane cloud forest trees. J Geophys Res 113:G03030. https://doi.org/10.1029/2007JG000613

Bagnouls B, Gaussen H (1957) Les climats biologiques et leur classification. Ann Georgr 355:193–220

Baker JCA, Santos GM, Gloor M, Brienen RJW (2017) Does Cedrela always form annual rings? Testing ring periodicity across South America using radiocarbon dating. Trees 31:1999–2009. https://doi.org/10.1007/s00468-017-1604-9

Borchert R, Calle Z, Strahler AH et al (2015) Insolation and photoperiodic control of tree development near the equator. New Phytol 205:7–13. https://doi.org/10.1111/nph.12981

Brand WA, Coplen TB, Aerts-Bijma AT et al (2009) Comprehensive inter-laboratory calibration of reference materials for $\delta^{18}O$ versus VSMOW using various on-line high-temperature conversion techniques. Rapid Commun Mass Spectrom 23:999–1019. https://doi.org/10.1002/rcm.3958

Breitsprecher A, Bethel J (1990) Stem-growth periodicity of trees in a tropical wet forest of Costa Rica. Ecology 71:1156–1164

Brienen R, Schöngart J, Zuidema P (2016) Tree rings in the tropics: insights into the ecology and climate sensitivity of tropical trees. In: Goldstein G, Santiago SL (eds) Tropical tree physiology. Springer, Geneva, pp 441–461

Callado C, Da Silva NS, Scarano F, Costa C (2001) Periodicity of growth rings in some flood-prone trees of the Atlantic Rain Forest in Rio de Janeiro, Brazil. Trees 15:492–497. https://doi.org/10.1007/s00468-001-0128-4

Calle Z, Schlumpberger BO, Piedrahita L et al (2010) Seasonal variation in daily insolation induces synchronous bud break and flowering in the tropics. Trees Struct Funct 24:865–877. https://doi.org/10.1007/s00468-010-0456-3

Cernusak LA, Ubierna N, Winter K et al (2013) Environmental and physiological determinants of carbon isotope discrimination in terrestrial plants. New Phytol 200:950–965. https://doi.org/10.1111/nph.12423

Cintra BBL, Gloor M, Boom A et al (2019) Contrasting controls on tree ring isotope variation for Amazon floodplain and terra firme trees. Tree Physiol 39:845–860. https://doi.org/10.1093/treephys/tpz009

David H, Díaz O, Urrea L, Cardona F (2014) Guía lustrada: Flora cañón del río Porce-Antioquia. EPM E.S.P. Universidad de Antioquia, Herbario Universidad de Antioquia

del Valle J (1994) Anotaciones sobre el clima de los bosques de guandal del delta del Rio Patía. Rev Fac Nac Agron 47:145–159

del Valle JI, Ramirez JA, Herrera DA (2012) Experiencias dendroclimáticas con árboles de ecosistemas contrastantes de Colombia. (Spanish). Cuad Geogr 21:117–126

del Valle JI, Guarín JR, Sierra CA (2014) Unambiguous and low-cost determination of growth rates and ages of tropical trees and palms. Radiocarbon 56:39–52. https://doi.org/10.2458/56.16486

Diaz JM, Gast F (2009) El Chocó Biogeográfico de Colombia. Banco de Occidente, Bogotá

dos Silva SM, de Assis F, Callado CH et al (2016) Growth rings in woody species of Ombrophilous Dense Forest: occurrence, anatomical features and ecological considerations. Braz J Bot. https://doi.org/10.1007/s40415-016-0313-8

Esquivel-Muelbert A, Baker TR, Dexter KG et al (2016) Seasonal drought limits tree species across the neotropics. Ecography (cop). https://doi.org/10.1111/ecog.01904

Evans MN, Schrag DP (2004) A stable isotope-based approach to tropical dendroclimatology. Geochim Cosmochim Acta 68:3295–3305. https://doi.org/10.1016/j.gca.2004.01.006

Faber-Langendoen D, Gentry AH (1991) The structure and diversity of rain forests at Bajo Calima, Choco Region, Western Colombia. Biotropica 23:2–11

Farquhar G, O'LearyBerry MJ (1982) On the relationship between carbon isotope discrimination and the intercellular carbon dioxide concentration in leaves. Aust J Plant Physiol 9:121–137

Fichtler E, Clark D, Worbes M (2003) Age and long-term growth of trees in an old-growth tropical rain forest, based on analyses of tree rings and ^{14}C. Biotropica 35:306–317. https://doi.org/10.1646/03027

Frankie G, Baker H, Oppler P (1974) Comparative phenological studies of trees in tropical wet and dry forests in the lowlands of Costa Rica. J Ecol 62:881–919

Fritts HC (1976) Tree rings and climate. Academic Press, New York

Giraldo JA, del Valle JI, Sierra CA, Melo O (2020) Dendrochronological potential of trees from America's rainiest region. In: Pompa-García M, Camarero JJ (eds) Latin American dendroecology. Springer International Publishing, Cham, pp 79–119

Goldsmith GR, Lehmann MM, Cernusak LA et al (2017) Inferring foliar water uptake using stable isotopes of water. Oecologia 184:763–766. https://doi.org/10.1007/s00442-017-3917-1

Green JK, Berry J, Ciais P et al (2020) Amazon rainforest photosynthesis increases in response to atmospheric dryness. Sci Adv 6:1–10. https://doi.org/10.1126/sciadv.abb7232

Groenendijk P, Sass-Klaassen U, Bongers F, Zuidema PA (2014) Potential of tree-ring analysis in a wet tropical forest: a case study on 22 commercial tree species in Central Africa. For Ecol Manag 323:65–68. https://doi.org/10.1016/j.foreco.2014.03.037

Guzmán D, Ruíz J, Cadena M (2014) Regionalización de Colombia según la estacionalidad de la precipitación media mensual, a través de análisis de componentes principales (ACP). Bogotá

Hazlett D (1987) Seasonal cambial activity for *Pentaclethra*, *Goelthasia* and *Carapa* trees in a Costa Rican lowland forest. Biotropica 19:357–360

Helle G, Schleser GH (2004) Beyond CO_2-fixation by Rubisco—an interpretation of $^{13}C/^{12}C$ variations in tree rings from novel intra-seasonal studies on broad-leaf trees. Plant Cell Environ 27:367–380. https://doi.org/10.1111/j.0016-8025.2003.01159.x

Herrera-Ramírez D, Sierra CA, Römermann C et al (2021) Starch and lipid storage strategies in tropical trees relate to growth and mortality. New Phytol 230:139–154. https://doi.org/10.1111/nph.17239

Holdridge LR (1967) Life zone ecology. Tropical Science Center, Costa Rica

Huete AR, Didan K, Shimabukuro YE et al (2006) Amazon rainforests green-up with sunlight in dry season. Geophys Res Lett 33:2–5. https://doi.org/10.1029/2005GL025583

Ishibashi H, Terashima I (1995) Effects of continuous leaf wetness on photosynthesis: adverse aspects of rainfall. Plant Cell Environ 18:431–438. https://doi.org/10.1111/j.1365-3040.1995.tb00377.x

Karger DN, Conrad O, Böhner J et al (2017) Climatologies at high resolution for the earth's land surface areas. Sci Data 4:1–20. https://doi.org/10.1038/sdata.2017.122

Kato S, Loeb NG, Rose FG et al (2013) Surface irradiances consistent with CERES-derived top-of-atmosphere shortwave and longwave irradiances. J Clim 26:2719–2740. https://doi.org/10.1175/JCLI-D-12-00436.1

Lehmann MM, Goldsmith GR, Schmid L et al (2018) The effect of ^{18}O-labelled water vapour on the oxygen isotope ratio of water and assimilates in plants at high humidity. New Phytol 217:105–116. https://doi.org/10.1111/nph.14788

Lisi C, Fihlo M, Botosso PC et al (2008) Tree-ring formation, radial increment periodicity, and phenology of tree species from a seasonal semi-deciduous forest in southeast Brazil. IAWA J 29:189–207

Managave S, Ramesh R (2012) Isotope dendroclimatology: a review with a special emphasis on tropics. In: Baskaran M (ed) Handbook of environmental isotope geochemistry. Springer, Berlin, pp 811–833

Managave SR, Sheshshayee MS, Borgaonkar HP, Ramesh R (2010) Past break-monsoon conditions detectable by high resolution intra-annual $\delta^{18}O$ analysis of teak rings. Geophys Res Lett. https://doi.org/10.1029/2009GL041172

McCarroll D, Loader NJ (2004) Stable isotopes in tree rings. Quat Sci Rev 23:771–801. https://doi.org/10.1016/j.quascirev.2003.06.017

Mendivelso HA, Camarero JJ, Gutiérrez E, Castaño-Naranjo A (2016) Climatic influences on leaf phenology, xylogenesis and radial stem changes at hourly to monthly scales in two tropical dry forests. Agric for Meteorol 216:20–36. https://doi.org/10.1016/j.agrformet.2015.09.014

Menezes M, Berger U, Worbes M (2003) Annual growth rings and long-term growth patterns of mangrove trees from the Braganca Peninsula, North Brazil. Wetl Ecol Manag 11(10):233–242. https://doi.org/10.1023/A:1025059315146

Mesa OJ, Rojo JD (2020) On the general circulation of the atmosphere around Colombia. Rev La Acad Colomb Cienc Exactas Físicas y Nat 44:857–875. https://doi.org/10.18257/raccefyn.899

Moreno MM, del Valle JI (2015) Influence of local climate and ENSO on the growth of Abarco (*Cariniana pyriformis*) in Chocó, Colombia. Trees 29:97–107. https://doi.org/10.1007/s00468-014-1094-y

O'Brien JJ, Oberbauer SF, Clark DB, Clark DA (2008) Phenology and stem diameter increment seasonality in a Costa Rican wet tropical forest. Biotropica 40:151–159. https://doi.org/10.1111/j.1744-7429.2007.00354.x

Ohashi S, Okada N, Nobuchi T et al (2009) Detecting invisible growth rings of trees in seasonally dry forests in Thailand: isotopic and wood anatomical approaches. Trees Struct Funct 23:813–822. https://doi.org/10.1007/s00468-009-0322-3

Ohashi S, Durgante FM, Kagawa A et al (2016) Seasonal variations in the stable oxygen isotope ratio of wood cellulose reveal annual rings of trees in a Central Amazon terra firme forest. Oecologia 180:685–696. https://doi.org/10.1007/s00442-015-3509-x

Oksanen E, Lihavainen J, Keinänen M et al (2018) Northern forest trees under increasing atmospheric humidity. In: Cánovas FM, Lüttge U, Matyssek R, Pretzsch H (eds) Progress in botany. Springer, Berlin, pp 317–336

Parolin P, Ferreira F, Piedade MTF et al (2016) Flood tolerant trees in seasonally inundated lowland tropical floodplains. In: Goldstein G, Santiago L (eds) Tropical tree physiology adaptations and responses in a changing environment. Springer, Berlin, pp 127–148

Pons TL, Helle G (2011) Identification of anatomically non-distinct annual rings in tropical trees using stable isotopes. Trees 25:83–93. https://doi.org/10.1007/s00468-010-0527-5

Poussart PF, Evans MN, Schrag DP (2004) Resolving seasonality in tropical trees: multi-decade, high-resolution oxygen and carbon isotope records from Indonesia and Thailand. Earth Planet Sci Lett 218:301–316. https://doi.org/10.1016/S0012-821X(03)00638-1

Poveda GG, Mesa OJ (2000) On the existence of Lloró (the rainiest locality on Earth): enhanced ocean–land–atmosphere interaction by a low-level jet. Geophys Res Lett 27:1675–1678. https://doi.org/10.1029/1999GL006091

Prenger J, Ling PP (2001) Greenhouse condensation control: understanding and using vapor pressure deficit (VPD). The Ohio State University, Extension Fact Sheet AEX-804, Wooster, OH

Rahman M, Islam M, Gebrekirstos A, Bräuning A (2019) Trends in tree growth and intrinsic water-use efficiency in the tropics under elevated CO_2 and climate change. Trees 33:623–640. https://doi.org/10.1007/s00468-019-01836-3

Reimer PJ, Brown TA, Reimer RW (2004) Discussion: reporting and calibration of post-bomb ^{14}C data. Radiocarbon 46:1299–1304

Restrepo-Coupe N, da Rocha HR, Hutyra LR et al (2013) What drives the seasonality of photosynthesis across the Amazon basin? A cross-site analysis of eddy flux tower measurements from the Brasil flux network. Agric for Meteorol 182–183:128–144. https://doi.org/10.1016/j.agrformet.2013.04.031

Risi C, Bony S, Vimeux F (2008) Influence of convective processes on the isotopic composition ($\delta^{18}O$ and δD) of precipitation and water vapor in the tropics: 2. Physical interpretation of the amount effect. J Geophys Res Atmos 113:1–12. https://doi.org/10.1029/2008JD009943

Roden JS, Ehleringer J (2000) Hydrogen and oxygen isotope ratios of tree ring cellulose for field-grown riparan trees. Oecologia 123:481–489

Roden JS, Lin G, Ehleringer JR (2000) A mechanistic model for interpretation of hydrogen and oxygen isotope ratios in tree-ring cellulose. Geochim Cosmochim Acta 64:21–35. https://doi.org/10.1016/S0016-7037(99)00195-7

Schöngart J, Piedade MTF, Ludwigshausen S et al (2002) Phenology and stem-growth periodicity of tree species in Amazonian floodplain forests. J Trop Ecol 18:581–597. https://doi.org/10.1017/S0266467402002389

Schöngart J, Bräuning A, Barbosa A et al (2017) Dendroecological studies in the neotropics: history, status and future challenges. In: Amoroso M, Daniels L, Baker P, Camarero J (eds) Dendroecology. Ecological studies (analysis and synthesis), vol 231. Springer, Cham, pp 35–73

Schweingruber FH (1988) Tree rings. Kluwer Academic Publishers, Dordrecht

Schweingruber FH (2007) Wood structure and environment. Springer, Berlin

Siegwolf R, Lehmann M, Goldsmith G et al (2021) The dual C and O isotope—gas exchange model: a concept review for understanding plant responses to the environment and its application in tree rings. Authorea. https://doi.org/10.22541/au.163844646.68129291/v1

Steinhof A, Altenburg M, Machts H (2017) Sample preparation at the Jena ^{14}C laboratory. Radiocarbon 59:815–830. https://doi.org/10.1017/RDC.2017.50

Urrea V, Ochoa A, Mesa O (2019) Seasonality of rainfall in Colombia. Water Resour Res 55:4149–4162. https://doi.org/10.1029/2018WR023316

Van der Sleen P, Groenendijk P, Zuidema PA (2015) Tree-ring $\delta^{18}O$ in African mahogany (*Entandrophragma utile*) records regional precipitation and can be used for climate reconstructions. Glob Planet Change 127:58–66. https://doi.org/10.1016/j.gloplacha.2015.01.014

Van der Sleen P, Zuidema PA, Pons TL (2017) Stable isotopes in tropical tree rings: theory, methods and applications. Funct Ecol 31:1674–1689. https://doi.org/10.1111/1365-2435.12889

Voelker SL, Meinzer FC (2017) Where and when does stem cellulose $\delta^{18}O$ reflect a leaf water enrichment signal? Tree Physiol 37:551–553. https://doi.org/10.1093/treephys/tpx029

Wagner F, Rossi V, Stahl C et al (2012) Water availability is the main climate driver of neotropical tree growth. PLoS ONE 7:1–11. https://doi.org/10.1371/journal.pone.0034074

Walter H, Harnickell E, Mueller-Dombois D (1976) Climate-diagram maps of the individual continents and the ecological climatic regions of the Earth. Springer, Berlin

Werner RA, Brand WA (2001) Referencing strategies and techniques in stable isotope ratio analysis. Rapid Commun Mass Spectrom 15:501–519. https://doi.org/10.1002/rcm.258

Yan Y (2005) Inter tropical convergence zone (ITCZ). In: Oliver JE (ed) Encyclopedia of world climatology. Springer, Dordrecht, pp 429–432